Asymmetric Autocatalysis

DOI: 10.1002/anie.201203398

Observation of a Transient Intermediate in Soai's Asymmetric Autocatalysis: Insights from ^{1}H NMR Turnover in Real Time**

Timo Gehring, Michela Quaranta, Barbara Odell, Donna G. Blackmond, and John M. Brown**

The amplifying asymmetric autocatalysis of alkylzinc addition to aldehydes discovered by Soai and co-workers in 1995 remains the only effective example of this genre,[1,2] despite widespread continuing interest in asymmetric amplification, primarily in the context of studies probing the origin of biological homochirality.[3] The autocatalytic process is highly circumscribed, being effective only within a narrowly defined regime: only 2-substituted pyrimidin-5-als such as **1** function as reactant[4] and only di-isopropylzinc **2** functions as reagent. The active catalyst is thought to be a higher-order alkoxide species derived from alkoxide **3** and is normally generated in situ from the alcohol **4**. Significant advances in the period since the initial discovery include absolute asymmetric synthesis,[5,6] amplification from extremely low to high levels of enantiomer excess,[7] and initiation by diverse chiral entities or by isotopically chiral promoters.[8,9] Kinetic and spectroscopic studies have provided much information about the nature of the autocatalytic process, and kinetic and computational modeling have contributed to our understanding. To date, however, neither experimental observations of intermediate species, nor evidence of the nature of the catalytic entity, have been reported. Hence the molecular mechanisms by which amplifying autocatalysis occur are not yet properly understood.

We report the direct observation of active species during catalytic turnover in the Soai autocatalytic Zn alkylation by ^{1}H NMR spectroscopy. This work confirms the surprising dependence on reaction temperature reported previously and reveals the first temporal observation of an intermediate species present during the reaction, which is transient at 0 °C but stable below −20 °C. The species is observed from the onset of the accelerating phase of autocatalytic turnover. Our earlier kinetic work indicated an equilibrating reaction product, formed without selectivity between homo- and heterochiral dimers, for which only the homochiral form was catalytically active.[10] Further studies demonstrated that the reaction was first-order in catalyst, close to second-order in aldehyde, but zero-order in the zinc alkyl reagent.[11] NMR analysis showed that the preferred dimer $\mathbf{3a_2}$ (Scheme 1) is

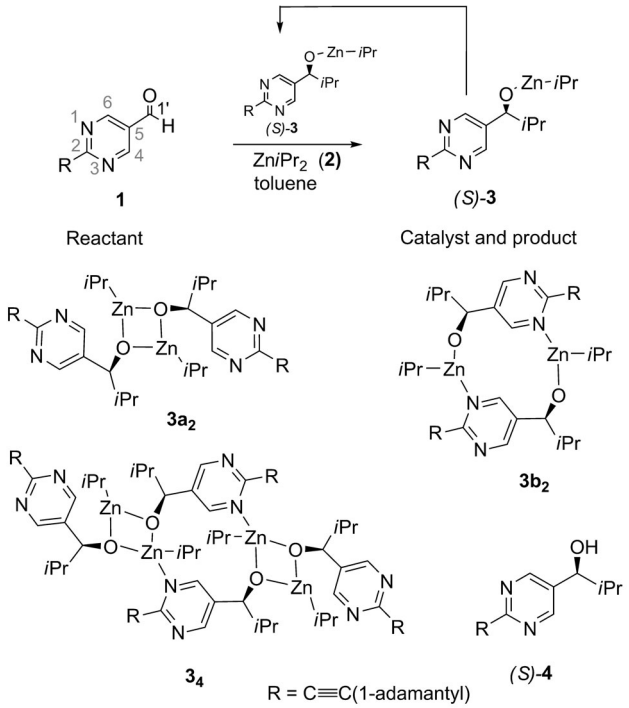

Scheme 1. Autocatalytic cycle for enantiomerically pure aldehyde **1**, and structures for product **3** and catalyst precursor **4**.

based on a $[Zn{-}O]_2$ square core and that the association of monomers is not stereoselective; the square dimer is also the one energetically preferred by DFT.[12] A mechanism based on an alternative macrocyclic form of the dimer $\mathbf{3b_2}$ as autocatalyst that binds two aldehydes and two alkylzincs prior to reaction has been successfully modeled by DFT calculations.[13] More recently, kinetic and NMR structural studies with aldehyde **1**[14] gave important new insights. Autocatalysis shows a strong negative Arrhenius effect in the temperature range −10 °C to 25 °C, with a rapid burst region following an induction period.[15] Concurrent NMR studies indicated a tetrameric alkoxide aggregate $\mathbf{3_4}$, with a postulated structure in line with prior DFT calculations.[16]

[*] Dr. T. Gehring, Dr. B. Odell, Dr. J. M. Brown
Chemistry Research Laboratory, University of Oxford
12 Mansfield Road, Oxford OX1 3TA (UK)
E-mail: john.brown@chem.ox.ac.uk
Dr. M. Quaranta
Imperial College of Science, Medicine and Technology
Department of Chemistry, London SW7 2AZ (UK)
Prof. D. G. Blackmond
Department of Chemistry, Scripps Research Institute
10550 N. Torrey Pines Rd., La Jolla, CA 92037 (USA)
E-mail: blackmond@scripps.edu

[**] This research was supported by EPSRC (D.G.B.), a Royal Society Wolfson Merit award (D.G.B.), NSF-ICC Award No. 1123895 (D.G.B.), and the Leverhulme Trust (J.M.B.). We thank NSCCS for computing facilities.

Supporting information for this article is available on the WWW under http://dx.doi.org/10.1002/anie.201203398.

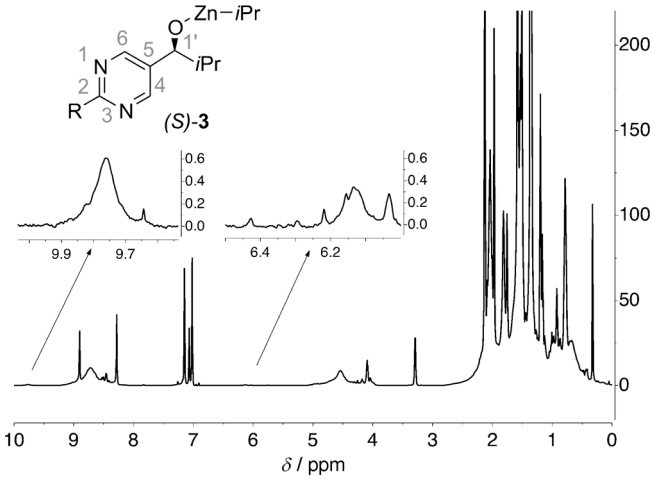

Figure 1. ^{1}H NMR spectrum of the reaction of **1** (0.022 M) with **2** (0.044 M); 0.5 mol% (*S*)-**4**, C_7D_8, 273 K, ca. 50% completion. Product (*S*)-**3** is at 8.6 ppm (H4,6) and 4.5 ppm (H1′). The transient is inset above (×65).

We first defined overall features of autocatalytic turnover by ^{1}H NMR spectroscopy at 0 °C, under conditions close to those employed in our recent work (Figure 1).[15] After rapid disappearance of the alcohol **4** with concurrent propane formation, an extended induction period with some loss of aldehyde signal is observed, followed by a rapid burst in reactivity that slows appreciably towards the end of the reaction, in agreement with our previous report.[15] The solution remains homogeneous throughout. The 8–10 ppm region is convenient for monitoring both aldehyde loss and product formation (Figure 1). Under these conditions the dynamically broadened pyrimidine H4,6 signal of product possesses $\omega_{1/2} \approx 140$ Hz at 700 MHz, unchanged over a concentration range of 0.013–0.025 M. This signal at 8.7 ppm is unsymmetrical and tails to beyond 9.5 ppm, independent of concentration. Initial analysis indicated smooth progression from reactant to product; on addition of Zn reagent **2** to aldehyde **1** the formyl and pyrimidyl protons broaden and shift upfield by up to 0.05 and 0.09 ppm, respectively. As reaction proceeds, the H4,6 and H1′ peaks of the reactant, and both CH and CH_3 peaks of **2** become increasingly deshielded (up to 0.04 ppm). In one run where excess **2** was removed by addition of further aldehyde **1**, the signals of the final product ^{1}H NMR spectrum were sharper at 25 °C than comparison samples containing residual **2**. This demonstrates rapid and reversible binding of the Zn reagent **2** to product **3**. Closer analysis of individual spectra in the 0 °C runs shows weak transient peaks at 9.7 and 6.1 ppm in 2:1 integral ratio that are not detectable before product is visible in the 8.7 ppm region. A shoulder at 8.6 ppm is also seen whilst the transient is visible. The proportion of the transient increases with increasing initial [**1**] but it never accounts for more than 1–2% of the total signal. The concentration rises rapidly to a maximum in the region of maximum rate and then decays with a half-life of ca. 300 s (see Supporting Information).

At −20 °C, reactant signals broaden substantially and shift downfield before significant product **3** is formed. During turnover, the spectrum looks strikingly distinct from the final state with additional sharp peaks at 8.95 (2H) and 8.65 ppm (2H), and broader peaks at 9.75 (2H) and 6.15 (1H) ppm. The latter two correspond to the transient peaks seen in the 0 °C runs. The four transient peaks grow together in direct relation to decay of aldehyde **1** and are stable for 1 h after complete consumption of **1**, in contrast to their rapid decay at 0 °C. (Figure 2). After warming to room temperature for several minutes and recooling to −20 °C, the spectrum shows complete loss of the transients and the equilibrium spectrum of **3** is restored. By FID subtraction of the ^{1}H NMR spectra taken at −20 °C directly before and after warming, the resulting difference spectrum clearly reveals the aforementioned four peaks in the 6–10 ppm region associated with the transient species, and liberation of aldehyde **1** (Figure 3).

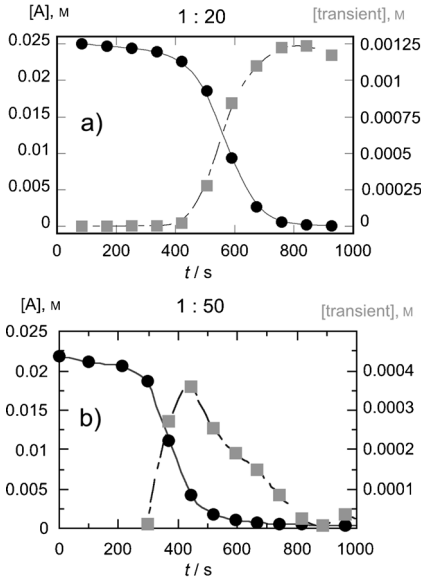

Figure 2. Above: The decay of aldehyde **1** (●), and the concurrent formation of transient species (■): a) at −20 °C and b) at 0 °C monitored by changes in the 6.1 ppm region. The transient signal is scaled up 20-fold for (a) and 50-fold for (b).

In order to characterize this novel intermediate further by NMR spectroscopy, a reaction was conducted between −50 and −40 °C, again with relatively high catalyst concentration (0.04 M **1**, 0.013 M **3**, 0.068 M **2**, C_7D_8). When the reactant had been consumed (ca. 20 min) the HSQC spectrum was recorded. This linked the ^{1}H signal H1B′ of the transient at 6.1 ppm with a ^{13}C resonance at 93 ppm, characteristic of an acetal (Scheme 2, and Supporting Information).[17] The observation is consistent with direct addition of a dimeric unit of Zn alkoxide **3** to aldehyde **1**, a process that is reversed on warming to room temperature as shown by the loss of the characteristic ^{1}H signals and the regeneration of **1**. The difference spectrum shown in Figure 3, together with analysis of the contributing spectra, reveals that the core fragment of the acetal incorporates two alkoxides and one aldehyde; however, one of the pyrimidine resonances at 8.95 ppm does not show cross-peaks to the other two subunits. From the Tr-

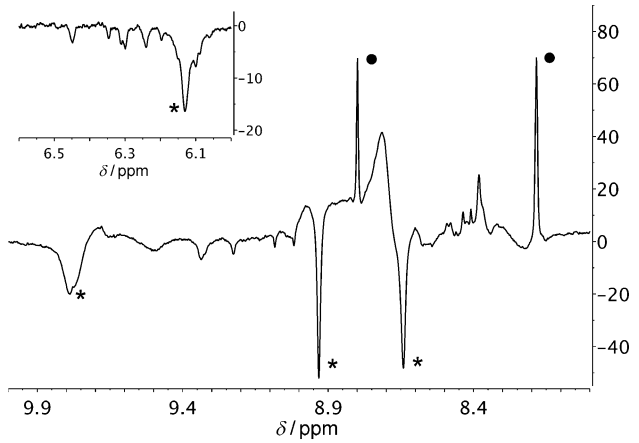

Figure 3. Difference spectrum from FID subtraction; completed reaction before and after warming from −20 °C to RT for 12 min. The acetal is seen as four inverted peaks ⁎; regenerated **1** is shown as ●.

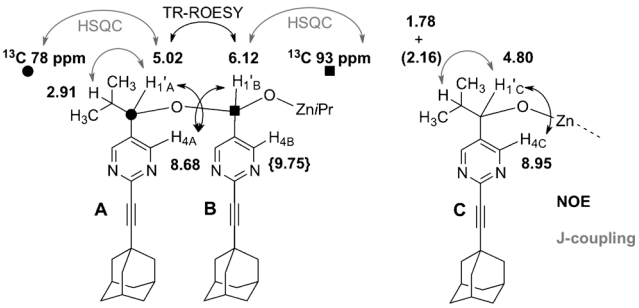

Scheme 2. Observations arising from 2D-NMR spectra of the acetal intermediate **5** at 233 K; the sharp peak at 8.95 ppm does not show relevant cross-peaks but always appears and disappears in concert, as does the broad signal at 9.75 ppm.

ROESY spectrum, the acetal proton at 6.12 ppm is linked to a single alkoxide proton at 5.02 ppm and both these have NOE's to the pyrimidine proton **A** at 8.68 ppm, thereby locating the formal acetal fragment as **A**,**B**. The 8.95 ppm pyrimidine peak, assigned as **C,** is linked in the Tr-ROESY to an alkoxide peak at 4.80 ppm but not directly to the acetal C–H. The 9.75 ppm peak is broad (possibly due to ring rotational dynamics) at −40 °C and consequently does not show any Tr-ROESY cross-peaks, and is thus designated to the pyrimidine C–H of the acetal **B**. Taking this evidence together permits assignment of the partial structure elements shown in Scheme 2. On completion of the analysis at −40 °C the sample was gradually warmed from −40 °C to 5 °C (5° steps, 8 min intervals). Rapid disappearance of the transient signals, with the formation of aldehyde **1** is observed as in the −20 °C experiment, but only at or above 0 °C.

The extent of formation of acetal **5** increases with initial concentration of aldehyde **1**, and increases even more dramatically with decreasing temperature. It is present in all runs with **1** at 0 °C and below, although the concentration remains very low in the 0.013 M run at 0 °C. The formal structure involves three distinct pyrimidine residues; on this basis estimates of maximum concentration during turnover are: 5 % at 0 °C, declining over time, 15 % at −20 °C, stable over time, for initial [A] = 0.025 M. At −40 °C ≥ 25 % of the new signal is associated with the acetal species **5**. Diffusion-ordered spectroscopy demonstrates that the relative mobilities of acetal **5** and product **3** at −40 °C are broadly similar (see Supporting Information).

The only previous recorded examples of acetal formation in Zn alkylations are intramolecular, involving $ZnEt_2$ and *o*-phthalaldehyde. Reaction in that case may be terminated after the first alkyl addition step by cyclization through a favorable 5-ring transition state, and the resulting hemiacetal may either be isolated or reacted further.[18] The observation of metalated hemiacetals in organometallic reactions is otherwise rare,[19] with a single X-ray characterization.[20] Hemiacetal intermediates have been implicated in catalysis, particularly in the Baylis–Hillman reaction.[21]

The structure of **5** is not revealed by NMR spectroscopy but the 2:1 ratio of alkoxide to aldehyde provides limitations. Preliminary DFT exploration of models arising from either the $(Zn–O)_2$ square form $\mathbf{3a_2}$ or the macrocyclic form $\mathbf{3b_2}$ produced feasible species **5a** and **5b;** the former requires rearrangement of an initial adduct to restore the $[Zn–O]_2$ core (Scheme 3). Without including additional $ZniPr_2$ bind-

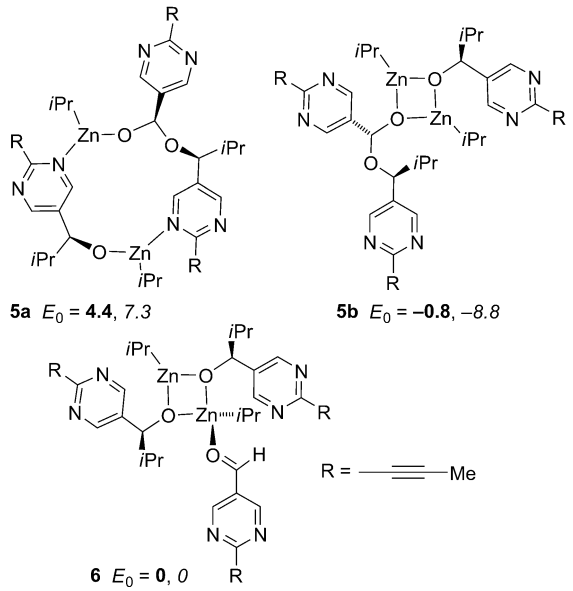

Scheme 3. Models for the structure of acetal **5** and adduct **6** arising from preliminary DFT calculations (B3-LYP; 6-31G(d,p); Zn/SDD, polarized continuum model (PCM) for toluene [bold]; or M06-2X; 6-31G(d,p); PCM for toluene [italics]); corrected for zero-point energy (ZPE). Energies are quoted in kcal mol^{-1} relative to adduct **6**.[22,23]

ing, structures **5a** and **5b** are respectively less and more stable than **6**, the Zn–O association complex between **1** and $\mathbf{3a_2}$ (see Supporting Information for details).

Experimental Section

Representative procedure: Stock solutions of (*S*)-**4** (1.1 mM, *ee* > 99 %) and freshly distilled $ZniPr_2$ (ca. 1 M, titrated vs. I_2/LiCl)[24,25] were prepared in [D_8]toluene. [**1**] = 0.013 M, 2.0 equiv $ZniPr_2$, 0 °C: An

oven-dried NMR tube was charged under N_2 with aldehyde **1** (2.1 mg, 7.9 μmol), [D_8]toluene (0.60 mL, dry, degassed), and the stock solution of (*S*)-**4** (4.0 μL, 0.040 μmol). An initial NMR spectrum was recorded in order to pre-optimize shimming parameters. The NMR tube was then cooled to 0 °C and Zn*i*Pr_2 (13.0 μL, 1.24 M, 16 μmol) was added. The time was noted and the NMR tube was capped, shaken, transported in the ice bath and loaded into the NMR machine (Bruker AV 700). The first NMR spectrum was recorded 4–6 min after Zn*i*Pr_2 addition, and subsequently through an automated pulse sequence (16 scans per record, 78 s interval between records). On completion of reaction the product *ee* was analyzed by HPLC (hexane/*i*PrOH gradient elution): at 0 °C, 0.013 M **1** 91 % *ee*, 0.017 M **1**, 94 % *ee*, 0.022 M **1**, 97 % *ee*, 0.025 M **1**, 94 % *ee*; at −20 °C, 0.025 M **1**, 94 % *ee*; at −40 °C, 0.047 M **1**, 94 % *ee*; at 0 °C, *rac*- catalyst, 0.017 M **1**, 4.5 % *ee*.

Received: May 2, 2012
Revised: July 3, 2012
Published online: August 31, 2012

Keywords: asymmetric catalysis · autocatalysis · NMR spectroscopy · Soai reaction · zinc

[1] K. Soai, T. Shibata, H. Morioka, K. Choji, *Nature* **1995**, *378*, 767–768.
[2] Asymmetric autocatalytic amplification, as a model for the origins of chirality in biology, had been mooted many years before: F. C. Frank, *Biochim. Biophys. Acta* **1953**, *11*, 459–463.
[3] Recent reviews: a) T. Gehring, M. Busch, M. Schlageter, D. Weingand, *Chirality* **2010**, *22*, E173–E182; b) T. Kawasaki, K. Soai, *J. Fluorine Chem.* **2010**, *131*, 525–534; c) K. Soai, T. Kawasaki, *Top. Curr. Chem.* **2008**, *284*, 1–33; d) I. D. Gridnev, *Chem. Lett.* **2006**, *35*, 148–153.
[4] a) T. Shibata, H. Morioka, S. Tanji, T. Hayase, Y. Kodaka, K. Soai, *Tetrahedron Lett.* **1996**, *37*, 8783–8786; b) T. Shibata, K. Choji, H. Morioka, T. Hayase, K. Soai, *Chem. Commun.* **1996**, 751–752.
[5] a) K. Soai, I. Sato, T. Shibata, S. Komiya, M. Hayashi, Y. Matsueda, H. Imamura, T. Hayase, H. Morioka, H. Tabira, J. Yamamoto, Y. Kowata, *Tetrahedron: Asymmetry* **2003**, *14*, 185–188; b) I. D. Gridnev, J. M. Serafimov, H. Quiney, J. M. Brown, *Org. Biomol. Chem.* **2003**, *1*, 3811–3819; c) D. A. Singleton, L. K. Vo, *Org. Lett.* **2003**, *5*, 4337–4339.
[6] Reviews on absolute asymmetric synthesis: a) B. L. Feringa, D. R. A. van Delden, *Angew. Chem.* **1999**, *111*, 3624–3645; *Angew. Chem. Int. Ed.* **1999**, *38*, 3418–3438; b) K. Mislow, *Collect. Czech. Chem. Commun.* **2003**, *68*, 849–864.
[7] I. Sato, H. Urabe, S. Ishiguro, T. Shibata, K. Soai, *Angew. Chem.* **2003**, *115*, 329–331; *Angew. Chem. Int. Ed.* **2003**, *42*, 315–317.
[8] Recent examples: a) T. Kawasaki, H. Ozawa, M. Ito, K. Soai, *Chem. Lett.* **2011**, *40*, 320–321; b) T. Kawasaki, S. Kamimura, A. Amihara, K. Suzuki, K. Soai, *Angew. Chem.* **2011**, *123*, 6928–6930; *Angew. Chem. Int. Ed.* **2011**, *50*, 6796–6798; c) T. Kawasaki, T. Sasagawa, K. Shiozawa, M. Uchida, K. Suzuki, K. Soai, *Org. Lett.* **2011**, *13*, 2361–2363; d) T. Kawasaki, M. Nakaoda, N. Kaito, T. Sasagawa, K. Soai, *Origins Life Evol. Biosphere* **2010**, *40*, 65–78; e) T. Kawasaki, Y. Hakoda, H. Mineki, K. Suzuki, K. Soai, *J. Am. Chem. Soc.* **2010**, *132*, 2874–2875.
[9] a) ^{13}C: T. Kawasaki, Y. Matsumura, T. Tsutsumi, K. Suzuki, M. Ito, K. Soai, *Science* **2009**, *324*, 492–495; b) ^{18}O: T. Kawasaki, Y. Okano, E. Suzuki, S. Takano, S. Oji, K. Soai, *Angew. Chem.* **2011**, *123*, 8281–8283; *Angew. Chem. Int. Ed.* **2011**, *50*, 8131–8133; c) ^{2}H: Ref. [8a], and earlier papers.
[10] D. G. Blackmond, C. R. McMillan, S. Ramdeehul, A. Schorm, J. M. Brown, *J. Am. Chem. Soc.* **2001**, *123*, 10103–10104.
[11] F. G. Buono, D. G. Blackmond, *J. Am. Chem. Soc.* **2003**, *125*, 8978–8979.
[12] I. D. Gridnev, J. M. Serafimov, J. M. Brown, *Angew. Chem.* **2004**, *116*, 4992–4995; *Angew. Chem. Int. Ed.* **2004**, *43*, 4884–4887.
[13] a) L. Schiaffino, G. Ercolani, *Angew. Chem.* **2008**, *120*, 6938–6941; *Angew. Chem. Int. Ed.* **2008**, *47*, 6832–6835; b) L. Schiaffino, G. Ercolani, *ChemPhysChem* **2009**, *10*, 2508–2515; c) L. Schiaffino, G. Ercolani, *Chem. Eur. J.* **2010**, *16*, 3147–3156; d) G. Ercolani, L. Schiaffino, *J. Org. Chem.* **2011**, *76*, 2619–2626.
[14] M. Busch, M. Schlageter, D. Weingand, T. Gehring, *Chem. Eur. J.* **2009**, *15*, 8251–8258.
[15] M. Quaranta, T. Gehring, B. Odell, J. M. Brown, D. G. Blackmond, *J. Am. Chem. Soc.* **2010**, *132*, 15104–15107.
[16] J. Klankermayer, I. D. Gridnev, J. M. Brown, *Chem. Commun.* **2007**, 3151–3153.
[17] Acetal resonances: a) M. Anteunis, G. Swaelens, J. Gelan, *Tetrahedron* **1971**, *27*, 1917–1929, and earlier papers; b) W. Migda, B. Rys, *Magn. Reson. Chem.* **2004**, *42*, 459–466.
[18] a) M. Watanabe, N. Hashimoto, S. Araki, Y. Butsugan, *J. Org. Chem.* **1992**, *57*, 742–744; b) K. Soai, Y. Inoue, T. Takahashi, T. Shibata, *Tetrahedron* **1996**, *52*, 13355–13362; c) H. Kleijn, J. T. B. H. Jastrzebski, J. Boersma, G. van Koten, *Tetrahedron Lett.* **2001**, *42*, 3933–3937.
[19] a) K. Asakawa, J. J. Dannenberg, K. J. Fitch, S. S. Hall, C. Kadowaki, S. Karady, S. Kii, K. Maeda, B. F. Marcune, T. Mase, R. A. Miller, R. A. Reamer, D. M. Tschaen, *Tetrahedron Lett.* **2005**, *46*, 5081–5084; b) A. Avenoza, J. H. Busto, J. M. Peregrina, *Tetrahedron* **2002**, *58*, 10167–10171.
[20] L. O. Müller, R. Scopelliti, I. Krossing, *Chimia* **2006**, *60*, 220–223.
[21] a) K. E. Price, S. J. Broadwater, H. M. Jung, D. T. McQuade, *Org. Lett.* **2005**, *7*, 147–150; b) K. E. Price, S. J. Broadwater, B. J. Walker, D. T. McQuade, *J. Org. Chem.* **2005**, *70*, 3980–3987; c) R. Robiette, V. K. Aggarwal, J. N. Harvey, *J. Am. Chem. Soc.* **2007**, *129*, 15513–15525.
[22] Gaussian 09; Rev C.1: M. J. Frisch et al., Gaussian, Inc., Wallingford CT, **2009**; see Supporting Information for full details.
[23] The added stability of **5b** in M06-2X calculations is due to the explicit treatment of dispersion that reveals [Zn−O]$_2$/pyrimidine attraction.
[24] A. Boudier, C. Darcel, F. Flachsmann, L. Micouin, M. Oestreich, P. Knochel, *Chem. Eur. J.* **2000**, *6*, 2748–2753.
[25] A. Krasovshiy, P. Knochel, *Synthesis* **2006**, 890–891.

